Available online at www.sciencedirect.com
SCIENCE DIRECT
Polymer 47 (2006) 2189–2197
polymer
www.elsevier.com/locate/polymer

Nematic phase formation of Boehmite in polyamide-6 nanocomposites

Ceren Özdilek, Eduardo Mendes, Stephen J. Picken *

Department of Polymer Materials and Engineering, Delft University of Technology, Julianalaan 136, 2826 BL Delft, The Netherlands

Received 4 October 2005; received in revised form 11 January 2006; accepted 12 January 2006

Abstract

Nematic phase behavior of titanate-treated Boehmite rods in a polyamide-6 matrix is reported. Optical polarization microscopy (OPM) and wide-angle X-ray scattering (WAXS) performed during heating and cooling cycles, are used to provide information on the level of orientation of Boehmite rods and polyamide-6 crystallites. The nematic orientation of Boehmite is clearly indicated by the permanent birefringence in OPM, which persists above the melting point of the polymer. The WAXS data show that the projection of Boehmite peaks on the 2D detector transform from isotropic to anisotropic as the Ti-Boehmite concentration is increased, regardless of temperature or the physical state of the polymer. Nematic order parameters are obtained by fitting a Maier–Saupe type function into the WAXS intensity curves. According to that, nematic order of the Boehmite peak increases gradually with the Ti-Boehmite content and it is unaffected by the heating–cooling cycles. As for the polyamide-6, nematic order of the γ-phase and one of the α-phase peaks decrease while that of the other α-phase peak increases with the number of cycles. Based on these observations, a structure for the colloidal liquid crystalline nanocomposite samples is proposed.

Keywords: Nematic phase; Boehmite; Critical concentration

1. Introduction

Most of the inorganic colloids, which exist in nature, are anisotropic particles. These are lyotropic systems, which show liquid crystalline order above a certain particle concentration (critical concentration, c^*). Colloidal Boehmite rods (γ-AlOOH) that are used in our studies illustrate a good example of an inorganic lyotropic system. Their aspect ratio (L/D) can have different values depending on the synthesis method. By using the hydrothermal synthesis method and the same aluminum precursors as in our study, aspect ratios in the range of 14–32 have been reported [1].

Boehmite dispersions have been studied extensively in terms of their phase behavior [2,3], dynamics [4] and rheology [5]. In addition to the studies in aqueous medium, they have been surface modified by various methods and have been investigated in a variety of organic solvents. In other examples, interaction of Boehmite particles with non-absorbing polymers has been described in detail [6,7].

In this paper, we focus on the nematic phase behavior of Boehmite rods in a polymer matrix, namely polyamide-6. In fact, the concept of liquid crystalline phases formed by inorganic particles in a polymer matrix is not entirely new. Some examples in literature describe the formation of ordered phases by clay minerals [8,9]. However, the phase behavior of Boehmite rods in a polymer matrix as well as its relation to the crystallization of the matrix has not been reported previously.

We have previously shown that Boehmite particles can be included in polyamide-6 by in situ polymerization to yield well-defined nanocomposites [10,11]. The present paper shows that the Boehmite rods retain their nematic order also in polyamide-6, although the critical concentration, c^*, is different than its value in aqueous medium. The formation of the nematic phase by Boehmite particles is generally described in terms of the Onsager model, which relates the critical concentration, c^* to the aspect ratio L/D ratio of the particles [12].

2. Experimental section

2.1. Boehmite rods

Boehmite rods were synthesized by using the method of Buining et al. [1,2]. This method used aluminium isopropoxide (Janssen) and aluminium tri-*sec* butoxide (Fluka) as the precursors. The synthesis of particles was described in more detail in our previous publications [10,11]. Boehmite

* Corresponding author. Tel.: +31 15 2786946; fax: +31 15 2787415.
E-mail address: s.j.picken@tnw.tudelft.nl (S.J. Picken).

0032-3861/$ - see front matter © 2006 Elsevier Ltd. All rights reserved.
doi:10.1016/j.polymer.2006.01.043

rods used in this study had an average length of 280 nm and average width of 20 nm, with 30% polydispersity.

2.2. Ti-Boehmite–ε-caprolactam mixtures

In order to study Boehmite rods in various systems, it was essential to apply a surface treatment to the rods against any irreversible aggregation. For this purpose, a titanate-type coupling agent was used: titanium IV, tris[2-[(2-aminoethyl)amino]ethanolato-O],2-propanolato (commercial name KR-44, Kenrich Chemicals) [13]. Boehmite rods were first transferred into *n*-propanol (Acros), into which the coupling agent was introduced. The final dispersions in *n*-propanol were mixed with ε-caprolactam and the solvent was completely evaporated. The mixture was separated into five test tubes, into which varying amounts of ε-caprolactam was added. In the end, stable dispersions of Ti-Boehmite in ε-caprolactam with the following concentrations were obtained: 0.53, 1.3, 2.6, 3.4, 4 and 5.2% (w/w).

2.3. Ti-Boehmite–polyamide-6 nanocomposites

The Ti-Boehmite–ε-caprolactam mixtures were used as precursors in the melt polymerizations. Polyamide-6 was produced via water initiated ring opening polymerization of ε-caprolactam [14,15].

The monomer, ε-caprolactam (Fluka) was used without further purification. The amounts of reactants were as follows: 40 g ε-caprolactam, 10 g aminocaproic acid (Aldrich), 0.25 g adipic acid (Fluka) and 10 ml water, as initiator. The reaction mixture was heated at 150 °C for 2 h to remove excess water, followed by polymerization at 230 °C during 4 h. After the reaction, the polymer product was subjected to Soxhlet extraction in methanol for 12 h, for the removal of monomeric and oligomeric species. In the end, polyamide-6 nanocomposites containing 1, 3, 5.5, 7, 9, 13 and 15% (w/w) Ti-modified Boehmite were obtained.

2.4. Sample preparation

The polymer samples were pressed into thin films by applying an approximate 180 kN force in a hydraulic press at 250 °C. The final thickness of films was about 0.3 mm. The films were extensively dried for several weeks in a vacuum oven at 80 °C before the characterizations were carried out.

2.5. Wide angle X-ray scattering (WAXS)

The amount of orientation in the nanocomposites was analyzed with an X-ray diffractometer D8-Discover from Bruker-Nonius. The sample holder was a home-built heating unit, which made possible to confine the polymer films between polyimide X-ray windows in a vertical position. The unit was connected to a thermo-couple and controlled by a fast-response power supply (maximum heating rate, 300 °C/min), which allowed a temperature range of 25–350 °C. The measurements were carried out using 0.154 nm Cu incident radiation. The scattering data was recorded on a 2D detector (1024×1024) and the sample to detector distance was 6 cm. Samples were subjected to heating–cooling cycles at a rate of 5 °C/min in the 180–240 °C interval and each cycle was paused at 30, 180 and 240 °C during a 1800 s data acquisition time.

2.6. Optical polarization microscopy (OPM)

Nanocomposite films that were confined between glass microscopy slides, were placed in a Mettler Toledo FP82HT hot stage to apply heating–cooling cycles between 180 and 240 °C at a rate of 5 °C/min. The samples could be followed real-time during the cycles by using a Nikon Eclipse E600 POL optical polarization microscope. Identical temperature intervals and heating rates were used in WAXS and OPM for making a direct comparison between the results. In addition, the sign of birefringence was determined by using a lambda plate as reference and examining if the birefringence in the samples was additive or subtractive. The difference between the lambda retardation along the two perpendicular optical axes in the sample indicated whether the overall retardation (or birefringence) is positive or negative.

2.7. Thermogravimetric analysis (TGA)

TGA was used to determine the Ti-Boehmite contents of the nanocomposites. The samples were heated from 25 to 800 °C at a rate of 50 °C/min and were held at 800 °C for 30 min. As the polymer degraded completely at this temperature, the residual weight was due to the inorganic content. The weight loss of freeze–dried Ti-Boehmite as measured in TGA was taken as reference.

3. Results and discussion

3.1. Phase behavior of Boehmite rods in ε-caprolactam

Ti-Boehmite dispersions in ε-caprolactam were investigated in terms of their phase behavior. When observed between

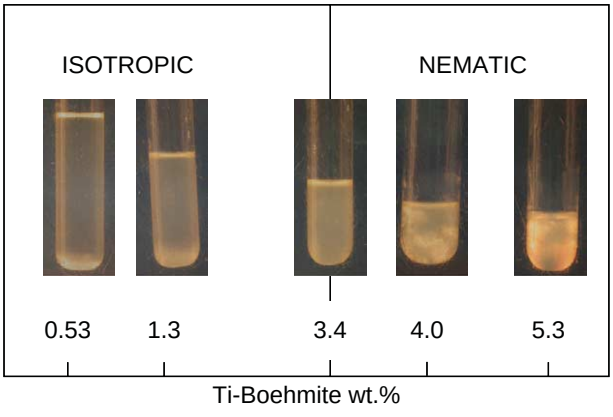

Fig. 1. Phase diagram of Ti-Boehmite in ε-caprolactam. The critical concentration is located at 3.4% (w/w).

crossed-polarizers, dispersions at 0.53 and 1.3% (w/w) concentrations were found to be isotropic (Fig. 1). The sample at 2.6% exhibited flow birefringence as the tube was shaken and the highest two concentrations, 4 and 5.2% exhibited permanent birefringence. In order to locate the critical concentration (c^*) with precision, one of the permanent birefringent samples was diluted with very small increments of ε-caprolactam. The point at which the sample turned from permanent to flow birefringent was determined as the c^* for the system. For the Ti-Boehmite rods in ε-caprolactam, the c^* value was found at 3.4% (w/w), which turned out to be very different than the c^* in aqueous medium (about 1%).

3.2. Phase behavior of Ti-Boehmite rods in polyamide-6 nanocomposites

The phase behavior of Ti-Boehmite rods in the polyamide-6 matrix was studied by optical polarization microscopy and X-ray scattering. However, in OPM studies, the observations were complicated by the presence of polyamide-6 crystallites since they contributed largely to the birefringence. One way to circumvent this problem was to work at temperatures above the melting point of polyamide-6. When polyamide-6 was completely in the melt, the permanent birefringence in OPM and the anisotropy in WAXS could be attributed only to the Ti-Boehmite particles.

3.2.1. Optical polarization microscopy (OPM)

According to the OPM analysis, all samples show certain amount of birefringence below the melting point of the polymer, because oriented polymer chains also give rise to birefringence (as discussed in Section 3.2). However, when the polymer starts to melt, all samples with concentrations of 5% and lower lose their birefringence and become completely isotropic. The samples with concentrations of 7% and higher retain their birefringence to some extent, even above the melting point. The optical microscopy results of the samples containing 7, 9, 13 and 15% Ti-Boehmite are shown in Fig. 2.

The images correspond to the state of the samples below and above the melting point of polyamide-6; at about 205 and 240 °C, respectively. In other obtain better results, the pictures at 205 °C are made with thin pressed samples and those at 240 °C are made with thicker samples. The reason for this is to improve the image quality above T_m where the birefringence becomes small.

Here, all of the samples are birefringent below T_m, although the effect is much stronger with the 13 and 15% samples. These samples also show the highest amount of birefringence above T_m, which is a clear indication of their nematic behavior. Compared to them, the 9% sample has somewhat lower birefringence (above T_m). As for the 7% sample, it does not become fully isotropic above T_m, but the amount of residual birefringence is still very low. As a result of the optical analysis, it can be concluded that the samples with Ti-Boehmite concentrations of 5% and lower are isotropic while 13 and 15% are nematic and the 7 and 9% samples should be in the biphasic region.

3.2.2. Wide-angle X-ray scattering (WAXS)

The samples were subjected to heating–cooling cycles as described in Section 2.6 and WAXS spectra were collected at 30, 180 and 240 °C. The spectra of the 5.5, 7, 13 and 15% samples in the last heating cycle are shown in Fig. 3. At 30 °C, the α-peaks of polyamide-6 and the two intense Boehmite peaks are clearly seen in all of the samples. At 180 °C, the two polyamide-6 peaks merge into one broad peak and finally transform into a diffuse melt phase peak at 240 °C, whereas the Boehmite peaks remain unaffected by the melting process. The general trend observed at all these temperatures is that the shape of the Boehmite scattering curves on the 2D detector transform from isotropic to anisotropic as Boehmite concentration is increased, being particularly strong at 13 and 15%. By performing heating–cooling cycles between 30 and 240 °C, it is proven that the Boehmite particles retain their orientation independent of the state of the polymer chains.

In Fig. 4a and b, intensity curves as a function of the scattering angle 2θ are shown. Fig. 4a illustrates the intensity curves of the samples with Boehmite concentration ranging from 1 to 15% and that of the unfilled polymer, obtained in the first heating cycle. Here, the α-peaks of polyamide-6 at 20.5 and 24° [16,17] are clearly seen in the unfilled polymer and in

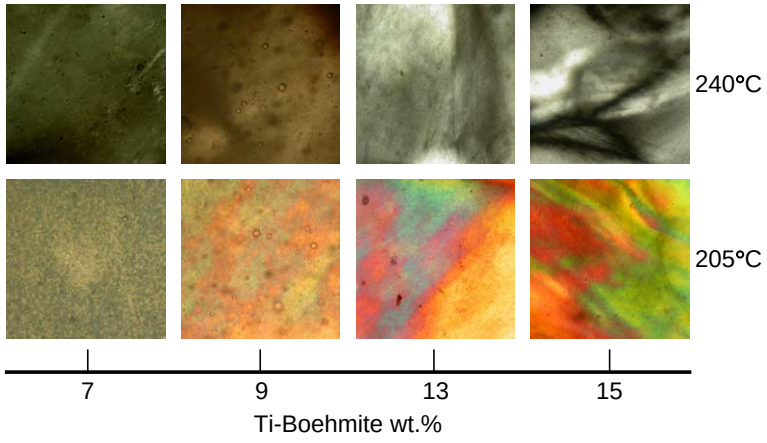

Fig. 2. OPM pictures of Ti-Boehmite-polyamide-6 nanocomposite samples at 205 and 240 °C.

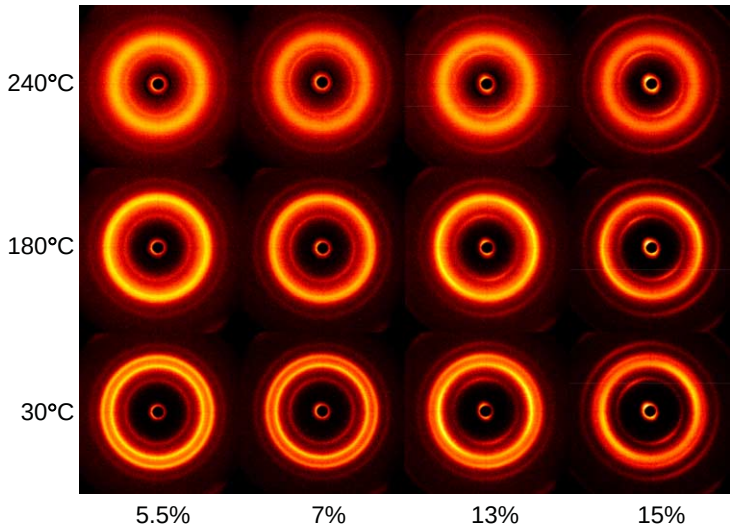

Fig. 3. Two-dimensional WAXS spectra of the 5.5, 7, 13 and 15% samples obtained at temperatures 30, 180 and 240 °C in the last heating cycle.

the nanocomposites. It is also known from literature that the γ-peak of polyamide-6 appears at 21.5° [16,17]. However, the presence of this peak is not obvious from Fig. 4a, since it is masked by the more intense neighbour, the first α-peak. In addition to these, the Boehmite peaks at 14 and 28° are observable throughout the whole concentration series.

Although not quite obvious for the 1% sample, the Boehmite peaks appear at 3% and become more intense with Boehmite concentration, as expected. Fig. 4b illustrates the intensity curves of the same samples as in Fig. 4a, obtained in the last heating cycle. Here, the α-peaks of polyamide-6 and the Boehmite peaks are present at all concentrations. The only difference with respect to Fig. 4a, is that the broad part between 20.5 and 24° is increased in intensity, which means that more of the γ-phase has formed during the heating–cooling cycles. Especially at 15% concentration, the peak at 21.5° is much more pronounced.

3.3. Determination of the nematic order parameter

The WAXS intensity curves as a function of the angle χ (chi) were fitted by a Maier–Saupe type function. The Maier–Saupe function used in the fitting procedure was the following [18,19]:

$$I = I_0 + A\, e^{\alpha \cos^2(\theta - \theta_0)}$$

The α-parameter obtained from the fitting was used to obtain the orientation distribution function, $F(\beta)$:

$$F(\beta) = \exp(\alpha \cos^2\beta)$$

By substituting the orientation distribution functions in the following integral, the average values of the nematic order

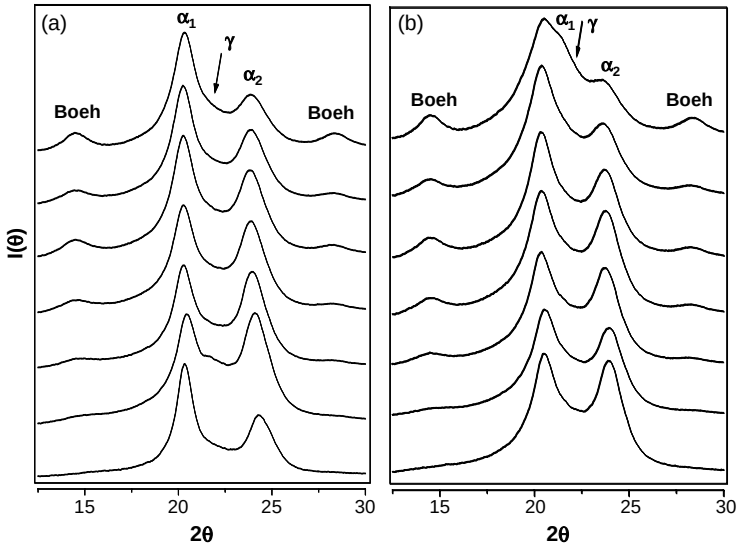

Fig. 4. WAXS intensity curves of the unfilled polyamide-6 and nanocomposites with 1, 3, 5.5, 7, 13 and 15% Ti-Boehmite (from bottom to top). (a) The first heating cycle. (b) The last heating cycle.

parameter could be calculated [18,19]:

$$\langle P_2 \rangle = \frac{\int_{-1}^{1} F(\beta) P_2(\cos\beta) \mathrm{d}\cos\beta}{\int_{-1}^{1} F(\beta) \mathrm{d}\cos\beta}$$

The intensity curves as a function of χ (chi) can be obtained for any 2θ value, making it possible to estimate the $\langle P_2 \rangle$ value for any peak. $\langle P_2 \rangle$ values of Boehmite and polyamide-6 peaks are determined separately in order to understand how the orientation of one species influences the other. Fig. 5a and b illustrates the $\langle P_2 \rangle$ parameters of the Boehmite peak at 14° with respect to the number of cycles, at temperatures of 30 and 240 °C, respectively. In these figures, all samples except the one with 1% concentration are included.

As seen in the figures for both temperatures, $\langle P_2 \rangle$ values gradually increase with the Ti-Boehmite content. In Fig. 5a, the 3 and 5.5% samples have certain $\langle P_2 \rangle$ values in the first cycle, but they decay to zero in the second and third cycles. This indicates that the macroscopic orientation in these samples is due to the polymer domains being oriented during the processing, so that after melting and recrystallization, the effect vanishes. When polyamide-6 is in the melt at 240 °C, the $\langle P_2 \rangle$ values of the 7, 9, 13 and 15% samples remain close to their initial values at 30 °C (Fig. 5b). Contrary to this, the 3 and 5.5% samples lose their orientation already in the first heating cycle and become completely isotropic in the melt. The plot at 240 °C clearly indicates that for concentrations of 7% and above, the source of nematic order in the system is the Ti-Boehmite particles, and not the polymer domains aligned in the sample processing.

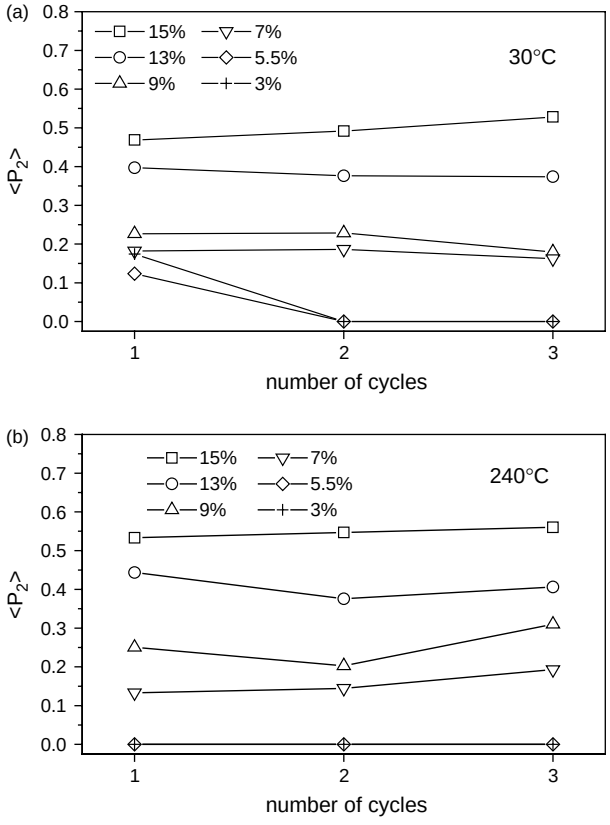

Fig. 5. (a) Nematic order parameter $\langle P_2 \rangle$ of Boehmite peak at 30 °C with respect to number of cycles. Ti-Boehmite concentrations are indicated by different symbols. (b) Nematic order parameter $\langle P_2 \rangle$ of Boehmite peak at 240 °C with respect to number of cycles. Ti-Boehmite concentrations are indicated by different symbols.

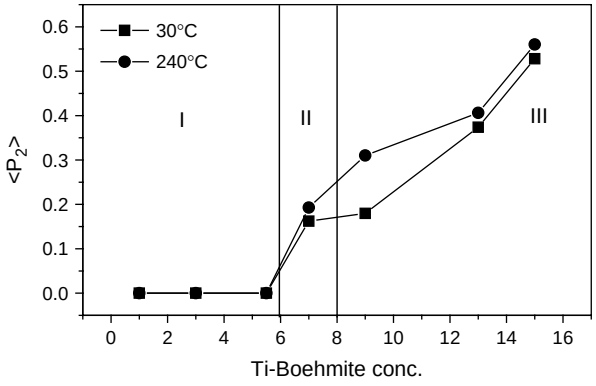

Fig. 6. Nematic order parameter $\langle P_2 \rangle$ of Boehmite peak as a function of Ti-Boehmite concentration at 30 and 240 °C. The regions are: I—isotropic, II—biphasic, and III—nematic.

By using the $\langle P_2 \rangle$ values of the Boehmite peak, it is possible to build a simple phase diagram. Fig. 6 shows the variation of $\langle P_2 \rangle$ with the Ti-Boehmite concentration in the nanocomposite samples. In order to exclude the orientation effects of the processing conditions, $\langle P_2 \rangle$ values obtained in the final cycle have been used. Once the effects of processing have been eliminated, it is observed that the $\langle P_2 \rangle$ values at 30 and 240 °C are almost identical. Mainly, three regions in the phase diagram can be distinguished: I—an isotropic region, where $\langle P_2 \rangle$ is zero; II—a very narrow biphasic region where the $\langle P_2 \rangle$ is non-zero, but still low; III—a nematic region where the $\langle P_2 \rangle$ values are much higher.

$\langle P_2 \rangle$ values of the polyamide-6 peaks have been obtained by applying the same procedure as in the treatment of Boehmite peaks. As discussed before, diffraction peaks of the α-phase of polyamide-6 appear at 20.5 and 24° and they will be referred to as α_1 and α_2, respectively. The diffraction peak of the γ-phase appears at 21.5°. For the fitting procedure, intensity versus χ curves have been plotted separately at 2θ values 20.5, 21.5 and 24°. However, the overlap between the α_1 and γ peaks (at 20.5 and 21.5°) makes it impossible to analyze them separately. Besides, the γ peaks do not have high intensity and they are masked by the higher intensity α_1 peaks. For these reasons, α_1 and γ peaks are analyzed together in all samples.

Fig. 7a shows the $\langle P_2 \rangle$ values for the $\alpha_1 + \gamma$ and α_2 peaks in the 15% sample as a function of number of cycles. From this figure, it is obvious that the nematic order of the $\alpha_1 + \gamma$ peak decreases with the number of cycles. Contrary to that effect, there is a significant increase in the nematic order of the α_2 peak. The 13% sample also shows similar behavior as the 15%, in the sense that $\langle P_2 \rangle$ for the combination of $\alpha_1 + \gamma$ decreases while that of the α_2 increases with the number of cycles. For the 7% sample, $\langle P_2 \rangle$ values of both the $\alpha_1 + \gamma$ peak and that of the α_2 peak decrease slightly with the number of cycles. Finally,

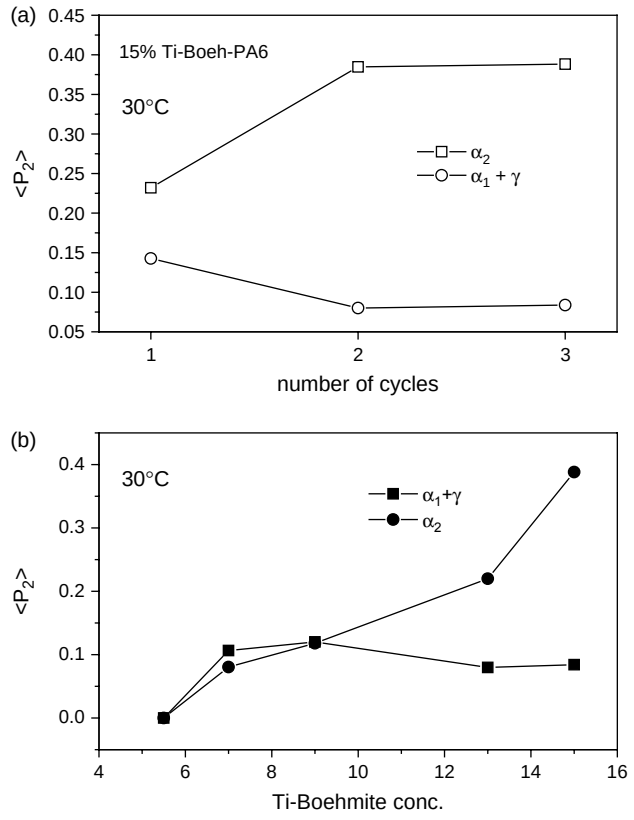

Fig. 7. (a) Nematic order parameter $\langle P_2 \rangle$ of $\alpha_1+\gamma$ and α_2 peaks in the 15% sample with respect to number of cycles. (b) Nematic order parameter $\langle P_2 \rangle$ of $\alpha_1+\gamma$ and α_2 peaks obtained in the last heating cycle as a function of Ti-Boehmite concentration.

for the 5.5, 3 and 1% samples, nematic order of the $\alpha_1+\gamma$ peak and that of the α_2 peak vanishes completely in the second and third cycles. This is also in agreement with our previous discussion that the orientation initially present in the isotropic samples is an effect of processing, which vanishes completely after melting and recrystallization.

To make the situation less complicated, the 15% sample is plotted as a function of number of cycles and for the rest of samples, only $\langle P_2 \rangle$ values obtained in the last heating cycle are shown. In Fig. 7b, $\langle P_2 \rangle$ values for the $\alpha_1+\gamma$ and the α_2 peaks in all samples are plotted as a function of Ti-Boehmite concentration. As seen in the figure, the nematic order of the α_2 peak has a tendency to increase and that of the $\alpha_1+\gamma$ peak has a tendency to decrease with the Ti-Boehmite concentration. This difference in behavior of the polyamide-6 peaks shows that the polymer chains have a preferential direction of orientation with respect to the Boehmite rods.

3.4. Structure investigation of the nanocomposites

In order to have better understanding of the structure of our nanocomposites and how orientation of one species affects the other, relative positions of Boehmite rods and polyamide-6 chains had to be determined. For this purpose, lattice plane information of Boehmite and polyamide-6 had to be extracted from the WAXS data. By using an excel-based program and the unit cell information on α-and γ-phases of polyamide-6 and Boehmite as taken from the literature [20–24], the lattice planes could be determined. Based on these lattice planes, the program yielded *d*-spacing and 2θ values, which were in complete agreement with the experimental values (Table 1).

Table 1
Unit cell parameters, *d*-spacing and 2θ values, and the corresponding lattice planes of polyamide-6 α- and γ-phases and of Boehmite

	Unit cell parameters*	*hkl*	*d*-spacing (nm)	2θ
Polyamide-6 α-phase	Monoclinic $a=0.96$, $b=0.80$, $c=1.72$, $\theta=112.5$	200	0.4416	20.11
		020	0.3700	24.05
Polyamide-6 γ-phase	Monoclinic $a=0.93$, $b=0.48$, $c=1.69$, $\theta=121.0$	200	0.3999	22.23
Boehmite	Orthorhombic $a=0.29$, $b=0.37$, $c=1.22$, $\theta=90.0$	002	0.6113	14.49
		004	0.3056	29.23

The values labeled with * are obtained from the literature.

In the literature, the α_1 reflection of polyamide-6 (20.5°) is assigned to the high electron density [200] inter-chain planes at a spacing of 0.44 nm [23]. The α_2 reflection (24°) corresponds to the [020] intersheet planes at a spacing of 0.37 nm. Similar to α_1, the γ reflection (21.5°) is due to the [200] inter-chain planes at a spacing of 0.40 nm [22]. The difference is that the γ-crystallites are made up of side-by-side packing of fully extended chains in the [200] plane. The unit-cell parameters of the γ-phase are also different from those of the α-phase (see Table 1). In the case of Boehmite, the 14 and 28° peaks are assigned to the [002] and [004] planes, respectively, which are the identical lattice planes [24].

By considering the lattice planes and the anisotropic 2D WAXS spectra (see Fig. 3), it is possible to propose a structure for the relative orientations of crystalline planes in the nanocomposites.

The orientations proposed in Fig. 8a give rise to the schematic WAXS spectrum as shown in Fig. 8b, which implies that the α_2 (020) direction lies parallel to the Boehmite (002) direction. The structure is constructed also by using the information from birefringence experiments. It is known that the maximum birefringence of polyamide-6 is along its long axis (*c* axis, normal to lamellar plane) [25]. Particles of anisotropic shape (like Boehmite rods) that are suspended in a medium with a different refractive index, show exclusively form birefringence and very little, if any, intrinsic birefringence [26]. In the case of rod-like particles, maximum polarization, and thus, birefringence occurs along the long axis of the rods [26]. Therefore, the sign of birefringence at different temperature intervals can be determined as described in Section 2.6, and it can give an idea on relative orientations of Boehmite rods and polyamide-6 lamella. Mainly, four different temperature intervals are investigated. According to the temperature, sources of birefringence are: I—at 180 °C,

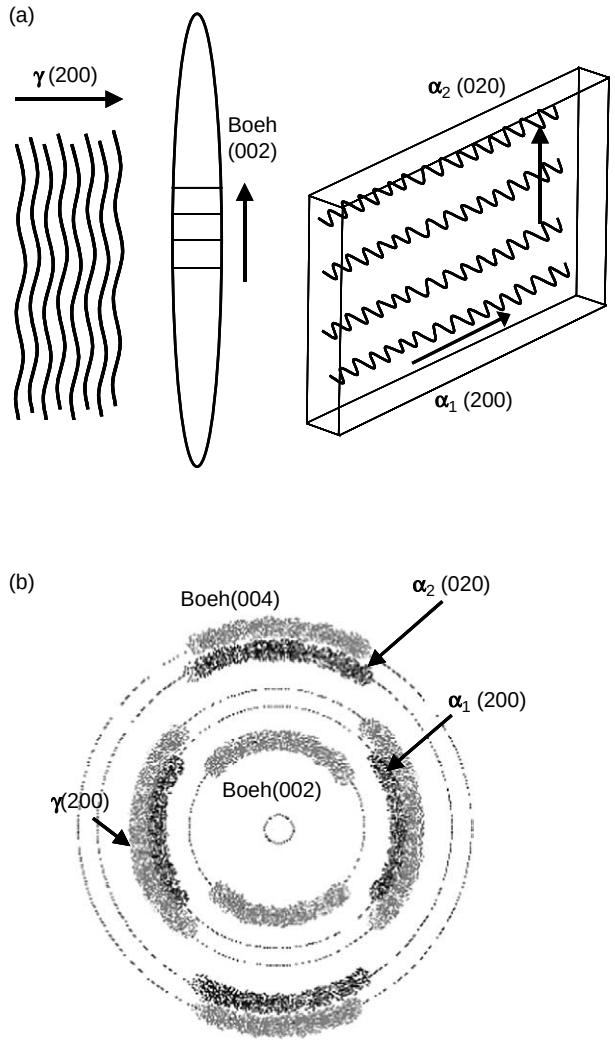

Fig. 8. (a) The structure proposed for the Ti-Boehmite–polyamide-6 nanocomposites. (b) The schematic WAXS pattern that should arise from the structure in (a).

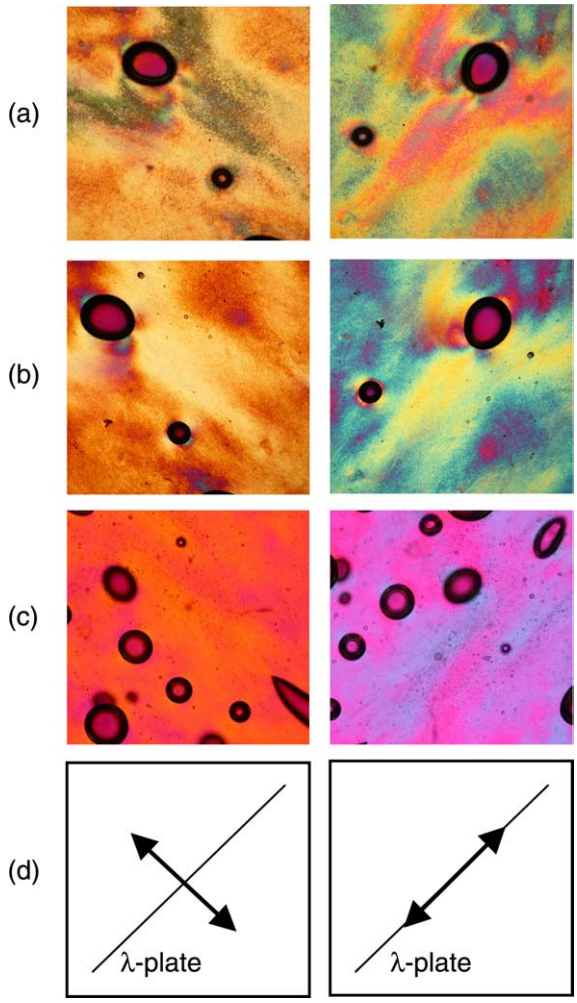

Fig. 9. Results of birefringence experiments made with the 13% sample at temperatures (a) 180 °C, (b) 212–216 °C and (c) 240 °C. (d) The arrow shows the direction of sample alignment with respect to the λ-plate.

Boehmite rods, γ- and α-crystals; II—at 210 °C, Boehmite rods, α-crystals and γ-phase in the process of melting; III—at 212–216 °C, Boehmite rods and α-phase in the process of melting; IV—at 240 °C, Boehmite rods in a complete polyamide-6 melt. The results of these experiments are summarized in Fig. 9.

Here, the birefringence results of the 13% sample at temperature intervals I, III and IV are shown. The results from interval II (210 °C) are not included because they are identical to those of interval III (212–216 °C). As explained earlier in Section 2.6, a reference lambda plate is used to determine whether the birefringence in the samples shifts the reference wavelength to higher or lower wavelengths. The difference in wavelength shift along the two orthogonal optical axes gives an indication of the sign of birefringence in the samples. The fact that the overall birefringence in the samples does not change sign in the course of the cycle that goes from Boehmite $+\gamma+\alpha$ to Boehmite $+\alpha$ and then to Boehmite rods in the polymer melt, implies that the long axes of all species lie in the same direction. Parallel alignment of the γ-crystals with respect to Boehmite rods is in agreement with the structure in Fig. 9a. However, the proposed structure also implies that the α-lamellae normal lies perpendicular to the Boehmite rod-axis, which cannot be properly explained by these birefringence results.

If this is the case, then the contribution to birefringence from the α-lamella should be negative, and the overall birefringence should change its sign during the melting cycle. One possible explanation to our results can be that the main contribution to the overall birefringence comes from the γ-phase. In addition, the fact that the birefringence does not change its sign after the melting of the γ-phase can be explained by a simple morphological picture (Fig. 10). Here, Boehmite rods are surrounded by the α-crystals to some extent, while the γ-phase regions are distributed between them. When the γ-phase is completely in the melt, α-crystals act as physical cross-links and hold the structure together, so the birefringence is still dominated by the oriented γ-phase.

But then, the morphological picture does not explain how the γ-phase, which is claimed to be the minor phase with a low $\langle P_2 \rangle$ can dominate the birefringence in the samples. In fact, the

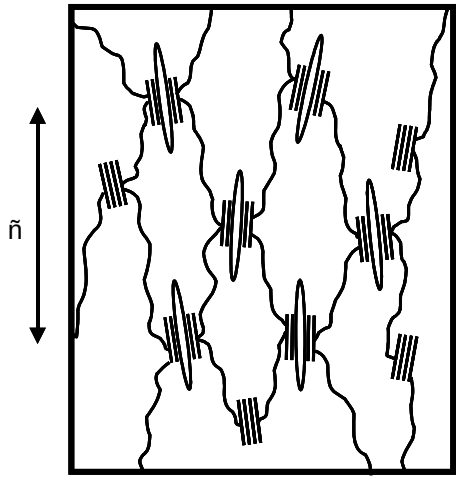

Fig. 10. The morphology proposed for the Ti-Boehmite–polyamide-6 nanocomposites. The nematic director ñ is indicated by the arrow.

total birefringence in the samples is somewhat complicated to analyze, since it contains four different contributions:

(1) Boehmite form birefringence, which is a small positive contribution as observed in separate refractometry experiments. This contribution becomes mainly important above all the melting points. It can be expressed as:

$$\Delta n,\ \text{Boeh} = \text{vol.fr.Boeh} \times \langle P_2 \rangle \text{Boeh} \times \Delta n_{\max} \text{Boeh}$$

(2) Positive contribution from the γ-phase with rather low $\langle P_2 \rangle$, which is expressed as:

$$\Delta n, \gamma = \text{vol.fr.}\gamma \times \langle P_2 \rangle \gamma \times \Delta n_{\max} \gamma$$

(3) Negative contribution from the α-lamella, which are attached to the Boehmite surface. In this case, the expression becomes:

$$\Delta n, \alpha = -1/2\{\text{vol.fr.}\alpha \times \langle P_2 \rangle \alpha \times \Delta n_{\max} \alpha\}$$

The factor $-1/2$ comes from the perpendicular orientation of the α-lamella with respect to the overall orientation direction [25].

(4) Contribution from the amorphous phase, which is distributed randomly throughout the sample. Although the amorphous phase is not oriented very well, it should still give an important positive contribution to the birefringence. The expression is:

$$\Delta n, \text{amorphous} = \text{vol.fr.amorphous} \times \langle P_2 \rangle \text{amorphous} \times \Delta n_{\max} \text{amorphous}$$

When combined altogether, these four terms yield the total birefringence in the samples. Although the level of orientation is an important factor, the fact that the exact volume fraction of each species is unknown (except that of Boehmite) complicates the situation and makes it very difficult to make quantitative conclusions based on birefringence experiments.

In the end, the birefringence results are in line with our morphological picture if we assume the matrix-continuum to be mainly of γ- and amorphous phases. Analyzing the birefringence yields interesting information on the level of orientation of various phases, but on the other hand it is very difficult to make quantitative conclusions. In this respect, the WAXS results are considered more reliable in determining the orientation and relative amounts of the α- and γ-phases.

4. Conclusions

We describe the nematic phase behavior of Boehmite rods in a polymer matrix for the first time. Ti-Boehmite–polyamide-6 nanocomposites are the materials used in the phase studies and their synthesis have been described in our previous publications. With Ti-Boehmite rods, the critical concentration to form the nematic phase, c^*, is determined as 3.4% (w/w) in the monomer ε-caprolactam and as 7% in polyamide-6. These values are different from the c^* in aqueous medium, which is 1% (w/w). During optical microscopy studies, there is large contribution to the birefringence from the oriented polymer chains. The best way to relate the birefringence in the samples to the nematic behavior of Boehmite is to analyze the samples above the melting point of polyamide-6. Another way to characterize the nematic phase behavior is through WAXS studies. Experiments performed at different temperatures show that WAXS patterns transform from isotropic to anisotropic as the Ti-Boehmite concentration is increased and that the Boehmite peaks are unaffected by the melting and crystallization processes of the polymer. Also the nematic order parameter $\langle P_2 \rangle$ of Boehmite increases systematically with the concentration. Information from two-dimensional WAXS spectra and lattice plane analysis of Boehmite and polyamide-6 are used to assign a general structure for the nanocomposites. According to that, the γ-crystals of polyamide-6 align parallel to the Boehmite rods while the α-lamellae normal lies perpendicular to the rod-axis. Additional birefringence measurements to confirm the general structure seem to be in conflict with the relative position of α-crystals. This conflict is explained by the fact that the overall birefringence in the samples should be dominated by the γ- and the amorphous phases.

Acknowledgements

The authors would like to thank Dr Liang-Bin Li for providing the heating set-up used in the WAXS experiments, and also for his useful discussions. This work forms part of the research program of the Dutch Polymer Institute.

References

[1] Buining PA, Pathmamanoharan C, Jansen JBH, Lekkerkerker HNW. J Am Ceram Soc 1991;74:1303.
[2] Buining PA. Preparation and properties of dispersions of colloidal Boehmite rods. PhD Thesis. Utrecht; 1992.
[3] Buining PA, Philipse AP, Lekkerkerker HNW. Langmuir 1994;10:2106.
[4] Van Bruggen MPB, Lekkerkerker HNW, Dhont JKG. Phys Rev E 1997; 56:4394.

[5] Wierenga A, Philipse AP, Lekkerkerker HNW. Langmuir 1998;14:55.
[6] Lekkerkerker HNW, Poon WCK, Pusey PN, Stroobants A, Warren PB. Europhys Lett 1992;20:559.
[7] Buitenhuis J, Donselaar LN, Buining PA, Stroobants A, Lekkerkerker HNW. J Colloid Interface Sci 1995;175:46.
[8] Lyatskaya Y, Balazs AC. Macromolecules 1998;31:6676.
[9] Ginzburg VV, Singh C, Balazs AC. Macromolecules 2000;33:1089.
[10] Ozdilek C, Kazimierczak K, Van der Beek D, Picken SJ. Polymer 2004;45:5207.
[11] Ozdilek C, Kazimierczak K, Picken SJ. Polymer 2005;46:6025.
[12] Onsager L. Ann NY Acad Sci 1949;51:627.
[13] Monte SJ. Polym Polym Compos 2002;10:1.
[14] Pielichowski J, Puszynski A. Polymer preparation methods. Krakow: Technical University of Krakow; 1978.
[15] Yasue K, Katahira S, Yoshikawa M, Fujimoto K. In: Pinnavaia TJ, Beall G, editors. Polymer-clay nanocomposites. New York: Wiley; 2000.
[16] Wu T, Liao C. Macromol Chem Phys 2000;201:2820.
[17] Liu X, Wu Q, Berglund LA, Qi Z. Macromol Mater Eng 2002;287:515.
[18] Picken SJ, Aerts J, Visser R, Northolt MG. Macromolecules 1990;23:3849.
[19] Viale S, Mendes E, Picken SJ. Mol Cryst Liq Cryst 2004;411:525 [1567].
[20] Mark JE. Physical properties of polymers handbook. Woodbury, NY: AIP Press; 1996.
[21] Holmes DR, Bunn CW, Smith DJ. J Polym Sci 1955;17:159.
[22] Arimoto H. J Polym Sci A 1964;2:2283.
[23] Atkins EDT, Hill M, Hong SK, Keller A, Organ S. Macromolecules 1992;25:917.
[24] Bokhimi X, Toledo-Antonio JA, Guzman-Castillo ML, Hernandez-Beltran F. J Solid State Chem 2001;159:32.
[25] Van Krevelen DW. Properties of polymers. 3rd ed. The Netherlands: Elsevier; 1997.
[26] Oldenbourg R, Salmon ED, Tran PT. Biophys J 1998;74:645.